Kinetics of Light Emission from XeI* Produced from Electron Beam Irradiation of Gaseous Mixtures of Xe and CF_3I

Franz Grieser and Hiroshi Shimamori*

Radiation Laboratory,† University of Notre Dame, Notre Dame, Indiana 46556 *(Received June 21, 1979)*

Publication costs assisted by the U.S. Department of Energy

The temporal characteristics of the light emission from XeI* B(1/2) state was studied following electron beam excitation of mixtures of Xe and CF_3I. Two processes were found to be responsible for the formation of the exciplex: (i) a nonionic sequence involving electronically excited states of xenon and ground state CF_3I; (ii) an ionic sequence with the main step probably being $Xe_2^+ + I^- \rightarrow XeI^* + Xe$. The deactivation rate constant of XeI* by CF_3I obtained from emission simulation results was determined to be $5 \pm 1 \times 10^{11}$ M^{-1} s^{-1}.

Introduction

The practical importance associated with the discovery of the rare gas–halogen exciplexes has been adequately demonstrated by the manufacture[1] of high-powered UV lasers utilizing these energetic species.

The reaction step usually ascribed[2] to the formation of the rare gas monohalides is

$$R^* + MX \rightarrow RX^* + M \qquad (1)$$

where R* is an electronically excited rare gas atom (metastable state) and MX a halogen (X) containing compound (M may also be a halogen).

An exception to reaction 1 was reported[3] for the formation of XeI* in electron beam excitation of Xe–I_2 mixtures. The results from this study were consistent with the process

$$Xe(^1S_0) + I_2^* \rightarrow XeI^* + I \qquad (2)$$

where I_2^* represents an electronically excited iodine molecule produced by the electron pulse.

In light of reaction 2 we were prompted to study other systems of Xe and iodine containing compounds. In the present work we report the kinetic processes responsible for the formation of XeI* in electron beam excitation of Xe–CF_3I mixtures, under experimental conditions similar to those of the Xe–I_2 study.[3]

Experimental Section

Xenon (Linde research grade, 99.995% purity) and CF_3I (Columbia Organic Chemicals, >95%) were purified by several freeze–pump–thaw cycles before use. All gas handling was conducted in a greaseless glass vacuum line.

The gas samples for irradiation were filled from the vacuum line via stainless steel Cajon O-ring fittings connecting the vacuum line to a 6.2 cm long cylindrical quartz cell. The windows of the cell were made of Suprasil 3.7 cm in diameter. When the desired pressure in the sample cell was attained, it was sealed with a greaseless Kontes Teflon stopcock.

The electron pulser used in this study was a 2.1-MeV Van de Graaff accelerator, with a maximum beam current of ~1.2 A in a 15-ns pulse. The irradiation was made on the side wall of the cylindrical cell, and the beam diameter at the wall was ~0.5 cm. The emission produced in the sample cell was monitored at right angles to the electron beam, reflected and focused through a series of mirrors and lenses, a radiation shielding wall, and into a Faraday cage. The light was then transmitted through a Bausch and Lomb monochromator (UV grating, band pass ~6 nm) and onto a 1P 28 photomultiplier, amplified, and displayed on a Tektronix 7904 oscilloscope. The trace on the screen was photographed with a polaroid camera using 10 000 ASA film. The rise time of the set up was <20 ns. The beam current (proportional to the input dose) was monitored by measuring the voltage drop at the terminal of the accelerator caused by the exit of the electron pulse. The intensity of the Čerenkov emission at 253 nm from a cell containing 435 torr of pure Xe was linearly related to the monitoring voltage.

Results and Discussion

The emission spectrum observed in the wavelength region of 240–400 nm following electron beam excitation of a Xe (~200 torr) and CF_3I (~0.2 torr) mixture was qualitatively the same as that observed in a pulse radiolysis study[3] of Xe–I_2 mixtures. Three emission bands were observed with emission maxima at ~253 nm (XeI* B(1/2) → XeI X(1/2)), ~320 nm (XeI* B(1/2) → XeI A(1/2)) and 345–350 nm[4] (I_2^* $^3\Pi_{2g} \rightarrow I_2$ $^3\Pi_{2u}$). The possibility that the latter band system was due to XeF*[5] or perhaps another band system[6] of XeI* was checked by irradiating samples of Xe/CH_2I_2 and Ar/CF_3I. In both cases the 345–350-nm band was still formed confirming the assignment of the emission to excited molecular iodine. The weaker XeI(C–A) band system previously observed[7,8] in the wavelength region 270 to 300 nm was not evident in the present work. This is not surprising since this band system is quite sensitive to the pressure of the inert gas[8] and would be expected to be reduced considerably with the xenon gas pressure (100–300 torr) used in the present study. The small amount of emission in the 270–300-nm region which we did observe (approximately 20 times smaller than the 253-nm maximum) may have some contribution from the C–A band but in itself does not interfere with the study of the kinetics of the more intense B–X band system at 253 nm.

The kinetics of the growth and decay of the emissions at 253 and 320 nm were the same under all the conditions of dose and gas pressures used; furthermore, the kinetics at other wavelengths within the two-band systems were the same as the emission maxima under the same experimental conditions. The similar behavior of the emission kinetics at 253 and 320 nm is of course expected since both these wavelengths monitor the deactivation of the lower

†The research described herein was supported by the Office of Basic Energy Sciences of the Department of Energy. This is Document No. NDRL-2025 from the Notre Dame Radiation Laboratory.

0022-3654/80/2084-0247$01.00/0

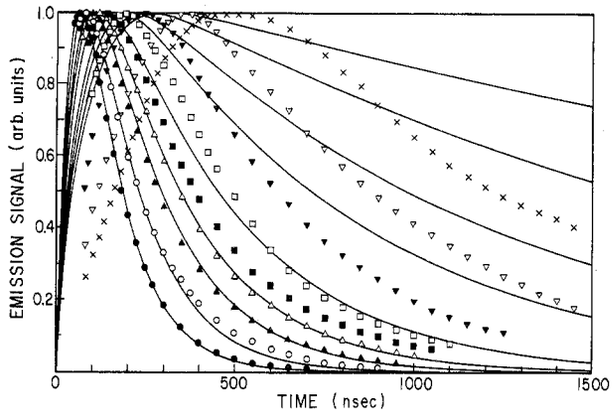

Figure 1. The temporal response of emissions from XeI* at 253 nm as a function of CF_3I pressure (●, 0.456 torr; ○, 0.342 torr; ▲, 0.248 torr; △, 0.197 torr; ■, 0.138 torr; □, 0.0748 torr; ▼, 0.0496 torr; ▽, 0.0272 torr, ×, 0.0136 torr). The pressure of Xe was kept constant at 210 torr. The relative electron dose was constant throughout this series. All the emissions have been standardized for comparisons of growth and decay kinetics. Solid curves are computer calculations based on the reaction scheme given in the text. These have been standardized to compare with experimental curves. The emission intensity during and somewhat after the electron pulse is not shown because Čerenkov light from the vessel obscured the initial portion of the emission trace.

vibrational levels of the XeI* B(1/2) state.[3]

On the other hand, kinetic behavior of the emission at ~350 nm was different from that observed at 253 or 320 nm. In particular, the growth rates were much slower. A similar difference in the kinetics between I_2* and the exciplex formations was also noted by previous studies with Xe–I_2[3] and Ar–CF_3I[9] mixtures. Our experiments were primarily directed at establishing the mechanism of formation of XeI* B(1/2) state under various conditions of irradiation dose and pressure of the two components, Xe and CF_3I. Therefore, little attention was directed at the I_2* formation processes.

The effect of CF_3I pressure on the growth and decay of the emission at 253 nm is shown in Figure 1. The data shown were taken from a number of oscilloscope traces and standardized to allow a better comparison of the emission kinetics at different CF_3I pressures. The solid curves are computer simulations; these will be discussed later. The initial signal growth during and somewhat after the pulse is not shown because of interference from Čerenkov light.

At CF_3I pressures ≳0.15 torr, no noticeable effect on the time of maximum intensity or decay rate of the emissions was observed with a change in either electron dose or xenon pressure (100–300 torr). Below ~0.15 torr of CF_3I, variation in the emission kinetics became significant with both dose and xenon pressure alterations. Lowering the dose by a factor of about 4 decreased the first-order decay rate of the emission by about 10–20% although the decay kinetics still remained first order at longer times. An example of such a dose effect is shown in Figure 2 for different CF_3I pressures (Xe pressure ~210 torr). Decreasing the Xe pressure also decreased the decay rate of the emission. This change is probably largely due to a change in the dose stopped by the system, since the emission kinetics were similar when the input electron dose was correspondingly lowered on a high-pressure xenon sample.

These effects of dose on the emission kinetics suggest that ionic species are precursors to XeI*, which become increasingly important at CF_3I pressures below ~0.15 torr. As will be seen later, the yield of XeI* at low CF_3I pressures is greater via the ionic pathway than the nonionic production.

Considering for the moment the XeI* formation at the higher CF_3I pressures, namely >0.15 torr, a simple reaction

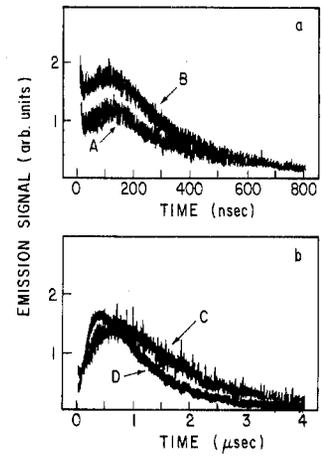

Figure 2. Effect of irradiation dose on the emission–time signals at 253 nm: (a) 210 torr of Xe + 0.193 torr of CF_3I; (b) 210 torr of Xe + 0.0141 torr of CF_3I. Relative dose was monitored by voltage drops at the beam ejection port of the accelerator. The voltages were 41, 160, 42, and 170 mV for curves A, B, C, and D, respectively. The vertical scales for curves A, B, and C have been amplified by 4, 1, and 10, respectively, relative to curve D.

scheme which would fit the experimental observations is the following.

$$Xe^* \text{ (or } Xe_2^*) + CF_3I \xrightarrow{k_1} XeI^* \text{ (or } XeI^* + Xe) + CF_3 \quad (3)$$

$$XeI^* \xrightarrow{k_2} h\nu + Xe + I \quad (4)$$

$$XeI^* + CF_3I \xrightarrow{k_3} \text{quenching} \quad (5)$$

The so-called "harpooning" reaction (3) is usually shown as involving the metastable rare gas atoms, i.e., $^3P_0$ and $^3P_2$ states. In the pulse radiolysis system there is no exclusive production of excited xenon species; however, with the Xe pressures used in the present study the major species which could be involved in the energy transfer reaction would be the low-lying metastable $^3P_0$, $^3P_2$ and resonance $^1P_1$, $^3P_1$ states of Xe. This is due to the rapid cascade, both by collisional and radiative processes, of higher energetic states. The resonance states of Xe have radiation lifetimes[10] of ~3 ns and would normally not be sufficiently long lived to participate in reaction 3; however, the high pressures of xenon used in this work facilitate the phenomenon of radiation trapping, resulting in dramatic lengthening of their lifetimes.

Le Calvé and Bourene[11] have discussed the case of predominant production of $Ar(^3P_2)$ following the electron beam excitation of argon gas. This may also be the case with xenon; however, since no direct evidence of the reacting state is available we have described the electronic state(s) simply as Xe*.

The xenon dimers (Xe_2*) formed by a 3-body process[12] ($k = 9.0 \times 10^9$ M^{-2} s^{-1}) are energetic enough to lead to the same products as Xe* on reaction with CF_3I. Since there was no pressure dependence (100–300 torr Xe) on the growth or decay rate of the XeI* emission, we must conclude that Xe_2* is equally as efficiently deactivated by CF_3I as Xe*.

Solving the differential equations associated with reactions 3–5 for the time-dependent concentration XeI*

$$\frac{d}{dt}([XeI^*]) = k_1[Xe^*][CF_3I] - k_2[XeI^*] - k_3[XeI^*][CF_3I] \quad (6)$$

$$[Xe^*] = [Xe^*]_0 e^{-k_1[CF_3I]t} \quad (7)$$

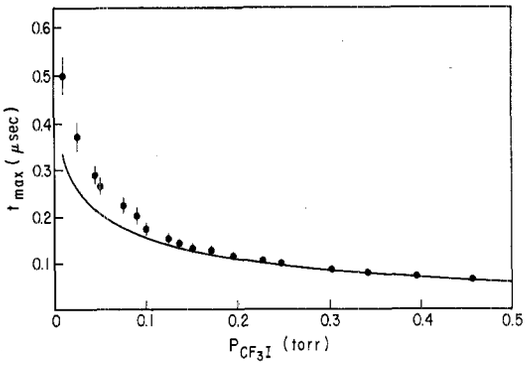

Figure 3. The variation of the time of emission maximum as a function of the CF_3I pressure. Conditions are the same as for Figure 1. The solid curve is the computer calculated t_{max} using eq 8 of text.

where $[Xe^*]_0$ is the initial amount of reactive xenon atoms present at the end of the electron pulse, gives

$$[XeI^*] = \frac{k_1[CF_3I][Xe^*]_0}{k_2 + k_3[CF_3I] - k_1[CF_3I]} (e^{-k_1[CF_3I]t} - e^{-(k_2+k_3[CF_3I])t}) \quad (8)$$

Equation 8 can also be used to obtain the time of maximum intensity t_{max} of the emission signal. This is

$$t_{max} = \ln\left(\frac{k_2 + k_3[CF_3I]}{k_1[CF_3I]}\right) \Big/ (k_2 + k_3[CF_3I] - k_1[CF_3I]) \quad (9)$$

Results of computer calculations based on eq 8 and 9 are shown with experimental data in Figures 1 and 3. A restriction used in the calculations was the radiative lifetime of XeI* B(1/2) which was found to be ~80 ns in another study.[3] As is seen, reasonably good fits to the experimental data could be obtained using the rate constants of $k_1 = 3.7 \times 10^{11}$ M^{-1} s^{-1} and $k_3 = 5 \times 10^{11}$ M^{-1} s^{-1}, for CF_3I pressures >0.15 torr. Below this pressure, where the ionic contribution to the formation of XeI* becomes noticeable, the calculated curves and those obtained experimentally become increasingly disparate.

The value of k_1 can be compared to the deactivation of $Xe(^3P_2)$ by CF_3I which was measured[13] as 3.2×10^{11} M^{-1} s^{-1}. The quenching constant k_3 is not readily comparable to other exciplex quenching reactions because they have not been widely studied. The only comparison we are aware of is the quenching of XeF* by several inert and halogen containing molecules.[14,15] The highest quenching constant[14] is for XeF_2 of 2.1×10^{11} M^{-1} s^{-1}.

The reaction sequence (3)–(5) can thus account for the observed emission kinetics with rate constants that seem reasonable for such reaction steps.

A comment should also be made regarding the radiative lifetime of the XeI* B(1/2) state. Hay and Dunning[16] have calculated that the lifetime of this state should be about 12 ns, considerably faster than the value we have used in our calculation. Using a value of 12 ns and the mechanism given by reactions 3–5 we could not obtain a satisfactory fit to the experimental data, particularly the time of maximum intensity. It is possible that the longer lifetime of 80 ns obtained in a previous kinetic study,[17] and which fits the present experimental data quite well, occurs because of xenon-induced equilibrium between the B(1/2) and C(3/2) state, as has been found for XeF* by Brashears and Setser.[15] It would be highly desirable to have a direct measurement of the lifetime of XeI* B(1/2) to resolve this point.

A method which had been used previously[3,17] to differentiate between the production of an emitting species via ionic and nonionic precursors was by the addition of a competitive electron scavenger. The amount of this scavenger is usually low such that it does not interfere with the deactivation of the nonionic processes normally occurring but sufficiently large enough to scavenge all the electrons such that the ionic sequence producing the emitting species is completely inhibited. We also attempted to do this by using SF_6 as a scavenger. However, the addition of a small amount (10% of CF_3I) of SF_6 to various Xe–CF_3I mixtures caused only a slight reduction (about 10%) of the emission intensities and did not change the kinetics. Dose alteration also gave no change in the kinetics between mixtures with SF_6 and those without SF_6. Apparently SF_6 cannot compete with CF_3I for electron capture. This may be due to either a higher electron capture cross section of CF_3I than the known value[18] or the much slower electron capture rate of SF_6 under the present conditions.[19] In any case it is clear that the procedure described above cannot differentiate between ionic and nonionic contributions to the emission. Thus, to gauge the importance of the ionic pathway of XeI* formation we used information from the time integrated emission (Y) over a range of CF_3I pressures (relative input dose, and xenon pressure being kept constant).

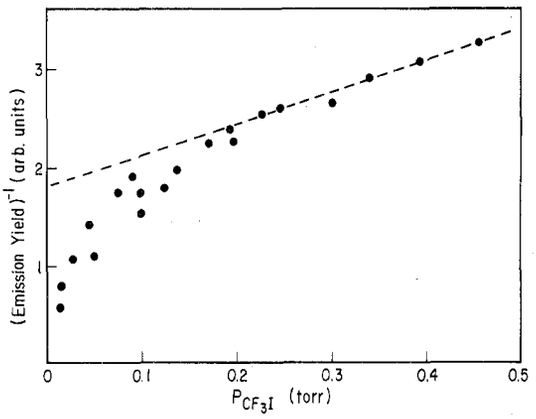

Figure 4. A plot of the reciprocal of the relative integrated emission time curves at 253 nm as a function of the CF_3I pressure. All conditions are the same for Figure 1. The dashed line represents a plot which would be expected if the emissions were produced by nonionic processes only.

In the CF_3I pressure region where the ionic contribution to the formation of XeI* is unimportant, the relationship

$$1/Y = \text{constant} \cdot (k_2 + k_3[CF_3I]) \quad (10)$$

derived from eq 8 shows that a plot of the recipocal of the relative integrated emission yield as a function of the CF_3I pressure should be linear. Figure 4 shows such a plot. The slope of the linear portion divided by the extrapolated intercept gives 3.2×10^4 M^{-1} which is equal to $k_3\tau_0$, where τ_0 is the XeI* radiative lifetime. Using 80 ns for τ_0 (ref 3) k_3 is found to be 4×10^{11} M^{-1} s^{-1}. This value compares favorably with the value obtained from the simulation results.

The point of deviation from linearity of the plot in Figure 4 is the beginning of the CF_3I pressure region in which the ionic pathway of XeI* production is important. From the extrapolated line shown in Figure 4 the amount of XeI* produced by the nonionic pathway can be estimated relative to the total amount of XeI* produced. The difference between the measured amount and that of the extrapolated quantity is of course the relative amount of XeI* produced by the ionic sequence. For example, at 0.04 torr of CF_3I, the relative total emission yield (Y) is ~1, whereas the relative nonionic yield would be ~$^1/_2$. Therefore, the relative ionic contribution is also ~$^1/_2$; i.e.,

equal ionic and nonionic contributions to the formation of XeI* are involved. At lower CF_3I pressures (<0.04 torr) the proportion of XeI* produced by the ionic pathway becomes even more important.

We shall now consider the ionic processes which must be present and which certainly influence the formation of XeI*. The Xe^+ ions produced by the electron pulse react efficiently with ground state xenon to give dimer ions[20] via

$$Xe^+ + 2Xe \rightarrow Xe_2^+ + Xe \qquad (11)$$

$$k = 7.2 \times 10^{10}\ M^{-2}\ s^{-1}$$

Two fates of Xe_2^+ are the ion–molecule and electron capture[21] steps

$$Xe_2^+ + CF_3I \rightarrow \text{products} \qquad (12)$$

$$Xe_2^+ + e \rightarrow Xe^* + Xe + KE \qquad (13)$$

$$k = 8.4 \times 10^{14}\ M^{-1}\ s^{-1}$$

Since CF_3I is quite an efficient electron scavenger, the latter reaction is not very important over the CF_3I pressure range studied.

The formation of I^- by the dissociative electron attachment process[18]

$$CF_3I + e \rightarrow I^- + CF_3 \qquad (14)$$

is important in the formation of XeI* probably by

$$Xe_2^+ + I^- \rightarrow XeI^* + Xe \qquad (15)$$

Energetically[22] the last step is possible by about 3 eV in forming the XeI* B(1/2) level (~5 eV, ref 6) and probably has a reaction rate constant of the order of 10^{14} to $10^{15}\ M^{-1}\ s^{-1}$. The electron capture reactions 13 and 14, although most efficient with thermal electrons, proceed with high energy electrons as well.

It was stated earlier that the decay rate of the XeI* emission at low CF_3I pressures still remained largely first order at longer decay times, which must mean one of the ion precursors to XeI* reacts in a pseudo-first-order step. A most likely process is reaction 12. An estimate of this reaction rate can be made from the "tail" of the low CF_3I pressure emission curves and works out as $6 \pm 1 \times 10^{11}\ M^{-1}\ s^{-1}$. This value is of the order one may expect from ion–molecule reactions.[23]

One further point to consider is why the ionic process forming XeI* is not important at high CF_3I pressures. This can be qualitatively understood from the ionic reaction steps considered above. The two main pathways for the reaction of Xe_2^+ are (12) and (15). At high CF_3I pressures reaction 12 predominates since the ion recombination reaction is relatively slow at the ion concentration formed by the pulse (we have estimated the ion concentration to be about 10^{-9} M using the method of Sauer and Mulac[24]). As the CF_3I pressure is lowered, however, reaction 15 becomes progressively more important. From some of Platzman's[25] calculations we could expect in the limit that the yield of XeI* through the ion mechanism would be about 2.5 times greater than the nonionic mode. This is based on the calculations that the species Xe^+ is 2.5 times more abundant than that of the excited atoms. Therefore, in the pressure regions where the scavenging steps of Xe_2^+ (and Xe^+) are minimal, the ionic pathway forming XeI* will predominate, and this is what is shown in the lower CF_3I pressure regions of Figure 4.

We have not attempted a simulation of the ionic reactions because of the overall complexity of the reaction mechanism involved, particularly the evolution of the high energy electrons as they degrade and are captured. Qualitatively, though, based on known rate constants of similar reactions the sequence described above is plausible.

Although we have not made a thorough investigation for the I_2* formation processes, it appears that both ionic and nonionic sequences are again responsible for its formation, because dose dependence as well as gas pressure dependence of the ~350-nm emissions behaved in a fashion similar to that observed from the XeI* emission.

Conclusions

Our results indicate that the production of XeI* occurs by at least two main processes, one involving the ground state of CF_3I and probably the lower electronic states of Xe, and the other an ionic sequence with the main step being $Xe_2^+ + I^-$. From computer fitting results of the emission–time curves of XeI* the rate constant for quenching of XeI* by CF_3I was determined as $5 \times 10^{11}\ M^{-1}\ s^{-1}$, which is in reasonable agreement with the value derived from the integrated emission–time curves.

Considering the results with the view of producing an efficient electrical discharge type XeI* laser, the best conditions would be with high ion densities and low concentrations of CF_3I, the latter to avoid scavenging of the ionic species Xe_2^+ and Xe^+. Perhaps not surprisingly, these observations seem to be the type of conditions employed in the commercially built exciplex laser systems such as KrF*, XeF*, and ArF*.

References and Notes

(1) For example, Tachisto Incorporated (U.S.A.) and Lambda Physik (West Germany) manufacture laser systems with the exciplexes ArF*, KrF*, XeF*, and KrCl*.
(2) For example: (a) J. E. Velazco and D. W. Setzer, *J. Chem. Phys.*, **62**, 1990 (1975); (b) S. K. Serles and G. A. Hart, *Appl. Phys. Lett.*, **27**, 243 (1975); (c) M. F. Golde and B. A. Thrush, *Chem. Phys. Lett.*, **29**, 486 (1974).
(3) R. Copper, F. Grieser, and M. C. Sauer, Jr., *J. Phys. Chem.*, **81**, 1889 (1977).
(4) Recent ab initio calculations by G. Das and A. C. Wahl, *J. Chem. Phys.*, **69**, 53 (1978), support the assignment given by previous researchers who had observed this iodine band.
(5) The emission maximum of the XeF* (B → X) transition is at 350 nm.
(6) C. A. Brau and J. J. Ewing, *J. Chem. Phys.*, **63**, 4640 (1975).
(7) J. H. Kolts, J. E. Velazco, and D. W. Setser, *J. Chem. Phys.*, **71**, 1247 (1979).
(8) M. P. Cassa, M. F. Golde, and A. Kvaran, *Chem. Phys. Lett.*, **59**, 51 (1978).
(9) F. Grieser, Ph.D. Thesis, University of Melbourne, 1976.
(10) (a) D. K. Anderson, *Phys. Rev.*, **137**, 21 (1965); (b) P. G. Wilkinson, *Can. J. Phys.*, **45**, 1715 (1967).
(11) J. Le Calve and M. Bourene, *J. Chem. Phys.*, **58**, 1446 (1973).
(12) R. Boncique and P. Mortier, *J. Phys.*, **D3**, 1905 (1970).
(13) (a) J. E. Velazco, J. H. Kolts, and D. W. Setser, *J. Chem. Phys.*, **65**, 3468 (1976); (b) *Ibid.*, **69**, 4357 (1978).
(14) R. Burham and N. W. Harris, *J. Chem. Phys.*, **66**, 2742 (1977).
(15) H. C. Brashears, Jr., and D. W. Setser, *Appl. Phys. Lett.*, **33**, 821 (1978).
(16) P. J. Hay and T. H. Dunning, Jr., *J. Chem. Phys.*, **69**, 2209 (1978).
(17) R. Cooper, F. Grieser, and M. C. Sauer, Jr., *J. Phys. Chem.*, **80**, 2138 (1976).
(18) Although the thermal electron capture rate constant of CF_3I has not been firmly established, the electron impact study (I. S. Buchelnikova, *Sov. Phys. JETP*, **8**, 783 (1959)) suggests that it is more than 100 times slower than the rate for SF_6 ($1.0 \times 10^{15}\ M^{-1}\ s^{-1}$).
(19) Considering that the thermalization of electrons may be very inefficient in collision with the main gas Xe, there is a possibility that CF_3I and SF_6 compete with each other for epithermal electrons, in which case it is expected that the electron capture cross section of SF_6 is considerably smaller than that for thermal electrons.
(20) A. P. Vitols and H. J. Oskam, *Phys. Rev. A*, **8**, 1860 (1973).
(21) H. J. Oskam and V. R. Mittlestadt, *Phys. Rev.*, **132**, 1445 (1963).
(22) This is based on electron affinity of I^- of 3 eV and an ionization potential (IP) for Xe_2 of 11 eV (IP(Xe) – $D(Xe_2^+)$). The dissociation energy of Xe_2^+ (1.1 eV) is from R. S. Mulliken, *J. Chem. Phys.*, **52**, 5170 (1970).
(23) (a) "Ion–Molecule Reactions in the Gas Phase", *Adv. Chem. Ser.*, **No. 58** (1966); (b) *Adv. Mass Spectrom.*, **2** (1963); **3** (1966).
(24) M. C. Sauer, Jr., and W. A. Mulac, *J. Chem. Phys.*, **56**, 4995 (1972).
(25) R. L. Platzman, *Int. J. Appl. Radiat. Isot.*, **10**, 116 (1961).